Performance of Piezoelectric MEMS Microphones

Author: Iwan Mohamed Jaber
Supervisor: Guillermo Villanueva

Course: EPFL semester project
Prof. Guillermo Villanueva

Lausanne, Spring semester 2018

ACKNOWLEDGEMENTS

Firstly, I would like to express my sincere gratitude to professor Guillermo Villanueva for placing his trust and confidence in my abilities to conduct this project. I would also like to thank him for his continuous support, patience and immense help. Without his precious knowledge and encouragements, it wouldn't have been possible to pursue this project.

Abstract

This semester project deals with the study of flat fully clamped plates with various geometries (circular and square), piezoelectric properties and uniformly distributed load (normal to the surface). The stress distribution is analyzed in order to obtain an electrical displacement. The objective is to distinguish positive and negative stresses areas in our plate in order to define an area for current measurements for microphone applications. For the circular plate, a straightforward analytical resolution of the problem is presented. For the square plate, the method of study is carried out mainly using the Galerkin method combined with the help of the symbolic algebraic software, Mathematica. The deflection of the plates is expressed in a series of polynomials which satisfy the homogeneous boundary conditions. Mathematica is used to solve for the coefficients and generating the trial functions. The stress of the plate is then determined. Then the results obtained are compared with the exact solution obtained with the use of the finite element analysis software, Ansys. The results obtained from the Galerkin method show good agreement with those from Ansys. Finally, the obtained stresses functions are analyzed to determine their positive/negative domains.

Contents

1 Introduction [2] [4]

1.1 Problem statement

We will take the example of the aeronautical field in order to introduce the stakes of our project. Cabin noise in flights is a main issue that every aircraft designer would like to reduce. One of the available solution to do so is the use of a distributed collection of microphones that spatially sample pressure fluctuations, enabling characterization of the turbulent boundary layer, identification of noise sources... This pressure fluctuation over our microphone can be illustrated by a model such as the one presented in figure 1.

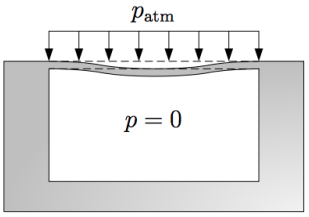

Figure 1: Pressure over the microphone [10]

A vacuum-sealed cavity is presented here and this particular case will be used in section 1.2 in order to define our problem modeling.

The use of microphones to sample those pressure fluctuations can be interesting since they convert sound into an electrical signal by utilizing a transduction mechanism.

In the above mentioned example, microphones should be as small as possible, thin, passive ans respond linearly to a large maximum pressure. Therefore, Piezoelectric transduction offers unique advantages over capacitive transduction such as simplicity of fabrication and linearity. This linear coupling between the mechanical stresses and the electrical response will be the main focus of our project.

In order to define precisely the problem we will solve across this project it is important to remind some basics about the piezoelectric principles.

The piezoelectricity existing in a given material can be explained in terms of its electric displacement (D) and strain (S), with respect to the stress applied (T) and the electric field generated (E) based on the following equations:

$$S_{ij} = s_{ijkl} T_{kl} + d_{kij} E_k \tag{1}$$

$$D_i = d_{ijk} T_{jk} + \varepsilon_{ij} E_j \tag{2}$$

where [d] is the matrix for the direct piezoelectric effect ,ε is permittivity and [s] is compliance under short-circuit conditions. The piezoelectric coefficient [d] has many elements but among which the most common modes are d_{31} (explains the electric polarization generated in a perpendicular direction to the applied stress) and d_{33}(explains the electric polarization generated in the same direction of the applied stress) as we will see in section 1.2.

We can see that if the electric field can be neglected in equation 2, we have an interesting linear relationship coupling the electric displacement with the mechanical stress applied.

Therefore, stress analysis at the design stage of a piezoelectric microphone can be utilized to optimize the location of the transduction electrodes to optimize the efficiency of the electrical detection, in other words, the coupled electrical response detected will increase with the coverage area of the electrodes as long as the polarity of the stress for every point covered by that area is identical due to piezoelectric properties presented above.

Indeed, for a piezoelectric transduction, a stack of a thin piezoelectric film sandwiched between two metal layers is generally used. The metallic electrodes are patterned to selectively apply an electrical potential across the film.

Thus, the objective of the project is to identify and distinguish positive/negative stresses in the microphones surface after applying an uniformly distributed load to optimize electrical detection. Indeed, by doing so, we will be able to increase the obtained measure by using an op-amp as illustrated in figure 2.

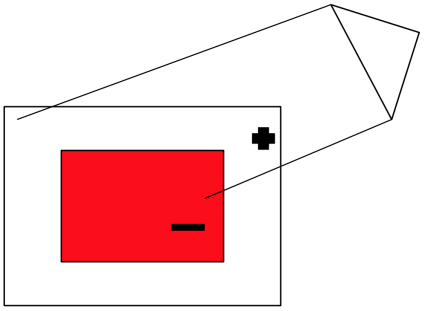

Figure 2: Optimized piezoelectric trans-ducted microphone

1.2 Assumptions

We will analyze across this project both circular/square plates to model the microphone and consider them in a polar/cartesian coordinate system as illustrated in figure 3.

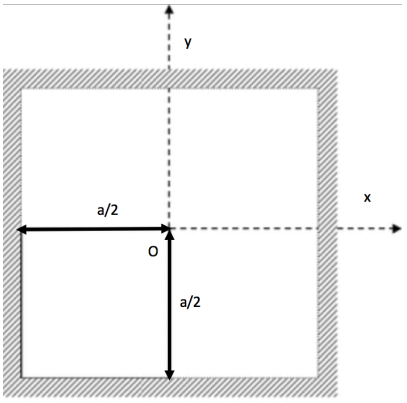

(a) Square plate coordinates

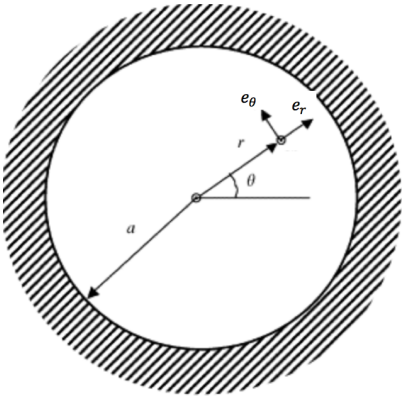

(b) Circular plate coordinates

Figure 3: Coordinate systems

The considered uniformly distributed load is applied on the top surface of the plate. Its intensity will be noted q (N/m^2) and the plates are considered fully clamped. This mechanical boundaries conditions are presented in figure 4.

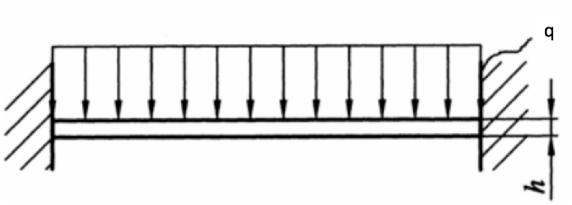

Figure 4: Side view of the considered plates with mechanical constraints

The anisotropic nature of materials such as most piezoelectric materials renders the analysis a bit more complex as several piezoelectric coefficients are available depending on the particular material cut and orientation. We therefore chose here to consider the isotropic case. The multilayer aspects of the different material chosen will be encompassed by the chosen numerical values of the material. Indeed, [11] showed that for a multilayer flatplate composed of a layer with a thickness t_a of material a and another layer of thickness t_b of material b we have equivalent flexural rigidity D_e and poisson ratio ν_e such as :

$$D_e = \frac{E_a t_a^3}{12(1-\nu_a^2)} K_{2p} \tag{3}$$

and:

$$\nu_e = \nu_a \frac{K_{3p}}{K_{2p}} \tag{4}$$

where:

$K_{2p} = 1 + \frac{E_b t_b^3 (1-\nu_a^2)}{E_a t_a^3 (1-\nu_b^2)} + \frac{3(1-\nu_a^2)(1+t_a/t_b)^2(1+E_a t_a/E_b t_b)}{(1+E_a t_a/E_b t_b)^2 - (\nu_a + \nu_b E_a t_a/E_b t_b)^2}$

and:

$K_{3p} = 1 + \frac{\nu_b E_b t_b^3 (1-\nu_a^2)}{\nu_a E_a t_a^3 (1-\nu_b^2)} + \frac{3(1-\nu_a^2)(1+t_a/t_b)^2(1+\nu_b E_a t_a/\nu_a E_b t_b)}{(1+E_a t_a/E_b t_b)^2 - (\nu_a + \nu_b E_a t_a/E_b t_b)^2}$

Finally, as presented in [9], if we can neglect the T_{33} compressive stress produced by the load q we can define a differential equation for the deflection w (for small deflections) of the plate for both circular and square plate:

$$\nabla^4 w = \frac{q}{D}, \forall (x,y) \in Area \tag{5}$$

where D is the flexural rigidity of the plate. Besides, the plate being considered fully clamped we have the following boundary conditions:

$$w(x,y) = 0, \frac{\partial w}{\partial n} = 0, \forall (x,y) \in \overline{Area} \tag{6}$$

NB: $\overline{Area}$ represents the lateral boundaries of the plate and $\widehat{n}$ is the normal vector of the lateral surface of the plate.

Besides, we know that for our elastic deformations:

$$D = \frac{Eh^3}{12(1-\nu^2)} \tag{7}$$

And:

$$T_{11} = \frac{-12Dz}{h^3}\left(\frac{\partial^2 w}{\partial x^2} + \nu \frac{\partial^2 w}{\partial y^2}\right), T_{22} = \frac{-12Dz}{h^3}\left(\nu \frac{\partial^2 w}{\partial x^2} + \frac{\partial^2 w}{\partial y^2}\right), T_{12} = \frac{-12Dz}{h^3}(1-\nu)\frac{\partial^2 w}{\partial x \partial y} \tag{8}$$

With h the plate thickness as represented in figure 4 and z the depth where we want to compute the stress. Besides, by using the notations : $11 \rightarrow 1, 22 \rightarrow 2, 33 \rightarrow 3, 23 \rightarrow 4, 13 \rightarrow 5$ and $12 \rightarrow 6$ we can transform equation2 such as:

$$\begin{bmatrix} D_1 \\ D_2 \\ D_3 \end{bmatrix} = \begin{bmatrix} 0 & 0 & 0 & 0 & d_{15} & 0 \\ 0 & 0 & 0 & d_{24} & 0 & 0 \\ d_{31} & d_{32} & d_{33} & 0 & 0 & 0 \end{bmatrix} \begin{bmatrix} T_1 \\ T_2 \\ T_3 \\ T_4 \\ T_5 \\ T_6 \end{bmatrix} + \begin{bmatrix} \varepsilon_{11} & 0 & 0 \\ 0 & \varepsilon_{22} & 0 \\ 0 & 0 & \varepsilon_{33} \end{bmatrix} \begin{bmatrix} E_1 \\ E_2 \\ E_3 \end{bmatrix}$$

Finally, by considering the previous assumptions and neglecting T_6 (it can be neglected as we will see in section 3) we end up with the following required stresses to get the main electrical displacement: $D_3 = d_{31}T_1 + d_{32}T_2$

And by assuming $d_{31} = d_{32}$ [3] (the symmetry elements of any physical property of a crystal must include the symmetry elements of the point group of this crystal. As a result, in tetragonal crystals of the 4mm symmetry, for example, there are only three independent components, and the piezoelectric effect is described by the matrix shown in the previous equation. If it acquires the $6mm$ symmetry, the poled ceramic has then $d_{31} = d_{33}$ we have finally:

$$D_3 = d_{31}(T_1 + T_2) \tag{9}$$

NB: Due to the isotropic properties of the piezoelectric effect matrix d, it does not change due to any rotation of the coordinate system and the same equation (9) can therefore be applied in a polar coordinate system as it has been shown in [6]. Indeed [6] states that for a 6mm crystal class, the piezoelectric relations are: $D_r = d_{15}T_{rz} + \varepsilon_{11}E_r, D_\theta = d_{15}T_{\theta z} + \varepsilon_{11}E_\theta$ and $D_z = d_{31}(T_{rr} + T_{\theta\theta}) + \varepsilon_{33}E_z$

And by using the same assumptions as before we will finally consider:

$$D_z = d_{31}(T_{rr} + T_{\theta\theta}) \tag{10}$$

Moreover, the previous statement has been computationally verified by computing the electrical displacements for the circular plate for both cartesian and polar coordinates in section 3.

Therefore, we will try throughout the next section to solve the differential equation (5) for the deflection since the finding of stresses and electrical displacements will then become straightforward by using (8) and (9).

2 State of the art

We will try to present across this section various methods to determine the deflection of the plate to solve our problem.

2.1 Circular plate

For the circular plate, the problem can be solved with an exact analytical solution that is obtained as follow.

Let's first remind the governing equation for deflection:

$$\nabla^2\nabla^2 w = \frac{q}{D}$$

In polar coordinates:

$$\nabla^2 w = \frac{1}{r}\frac{\partial}{\partial r}(r\frac{\partial w}{\partial r}) + \frac{1}{r^2}\frac{\partial^2 w}{\partial \theta^2} + \frac{\partial^2 w}{\partial z^2}$$

Moreover since we consider symmetrically loaded plate, $w = w(r) \Rightarrow$:

$$\nabla^2 w = \frac{1}{r}\frac{d}{dr}(r\frac{dw}{dr}) \Rightarrow \frac{1}{r}\frac{d}{dr}(r\frac{d}{dr}(\frac{1}{r}\frac{d}{dr}(r\frac{dw}{dr}))) = \frac{q}{D}$$

Therefore, by straight integration considering q constant and C_i the integration constants:

$$w(r) = \frac{qr^4}{64D} + C_1 ln(r) + C_2 \frac{r^2}{2} + C_3 \frac{r^2}{4}(2ln(r) - 1) + C_4 \tag{11}$$

And:

$$\frac{dw}{dr} = \frac{qr^3}{16D} + C_1/r + C_2 r + C_3 rln(r) + C_4 \tag{12}$$

Finally considering that for a circular plate (considering the coordinate system presented in figure 3) we must have a finite displacement at $r = 0 \Rightarrow C_1 = 0$ and due to the fully clamped edged we must have $w(a) = \frac{dw}{dr}(a) = 0$

$$\Rightarrow w(r) = \frac{q}{64D}(a^2 - r^2)^2 \tag{13}$$

And:

$$\frac{dw}{dr} = -\frac{qr}{16D}(a^2 - r^2) \tag{14}$$

Besides let's remind that for the in-plate displacements we have:

$$u_r(r) = -z\frac{dw}{dr}(r) \text{ and } u_\theta(r) = 0$$

This gives us the in-plane strains:

$$S_{rr} = \frac{du_r}{dr} = \frac{qz}{16D}(a^2 - 3r^2),\ S_{\theta\theta} = \frac{u_r}{r} = \frac{qz}{16D}(a^2 - r^2) \text{ and } S_{r\theta} = 0$$

Furthermore, knowing that:

$$T_{rr} = \frac{E}{1-\nu^2}(S_{rr} + \nu S_{\theta\theta}); T_{\theta\theta} = \frac{E}{1-\nu^2}(\nu S_{rr} + S_{\theta\theta}); T_{r\theta} = 0$$

And considering a thickness h as presented in figure 4 we have:

$$T_{rr} = \frac{3qz}{4h^3}((1+\nu)a^2 - (3+\nu)r^2); T_{\theta\theta} = \frac{3qz}{4h^3}((1+\nu)a^2 - (3\nu+1)r^2); T_{r\theta} = 0 \tag{15}$$

We thus have exact solutions that will be studied in section 3 in order to determine the sign of the electrical displacement D_z (see equation (10)) over the plate's area.

2.2 Square plate

Let's first present the governing equation for the displacement in cartesian coordinates:

$$(5) \Leftrightarrow \frac{\partial^4 w}{\partial x^4} + \frac{\partial^4 w}{\partial y^4} + 2\frac{\partial^4 w}{\partial x^2 \partial y^2} = \frac{q}{D} \tag{16}$$

This equation cannot lead to any exact analytical solution. We will therefore present approximated solutions that can be obtained for the deflection.

NB: The direct method of section 2.2.1 is presented here as an alternative solution to the variational method that was chosen to lead this project. It is important to note that we did not implement this method but a comparison involving the latter could have been interesting.

2.2.1 Direct method

The principle here is to use Fourier series to solve the PDE and then approximate the solution by taking a certain number of terms from the found infinite serie.

To obtain the serie mentioned above we procede as follow. We first solve the problem for a simply supported plate (no moment along edges) and we then superpose on the deflection of such a plate, the deflection of plate by moments distributed along edges. Both of those deflection respect $w = 0$ along edges. Thus, the moments have to be adjusted in such a manner to satisfy the condition $\frac{\partial w}{\partial n} = 0$ at the boundary of the clamped plate with: $w = w_1 + w_2$, where w_1 is the

deflection of the simply supported plate and w_2 is the deflection due to the moments distributed along edges.

We get from [9] that the deflection of a simply supported plate is represented (using the coordinates presented in figure 3) by:

$$w_1 = \frac{4qa^4}{\pi^5 D} \sum_{m=1,3,5...}^{\infty} \frac{(-1)^{\frac{m-1}{2}}}{m^5} cos\frac{m\pi x}{a}(1 - \frac{\alpha_m tanh\alpha_m + 2}{2cosh\alpha_m} cosh\frac{m\pi y}{a} + \frac{1}{2cosh\alpha_m}\frac{m\pi y}{a} sinh\frac{m\pi y}{a})$$

Where: $\alpha_m = m\pi/2$

We therefore have here a deflection depending on the materials parameters and

Besides we also get from [9] that the deflection w_2 caused by a moment $M_{x,y}$ for $x, y = \pm a/2$ is:

$$w_2 = -\frac{a^2}{2\pi^2 D} \sum_{m=1,3,5...}^{\infty} E_m \frac{(-1)^{\frac{m-1}{2}}}{m} cos\frac{m\pi x}{a}(\frac{m\pi y}{a} sinh\frac{m\pi y}{a} - \alpha_m tanh\alpha_m cosh\frac{m\pi y}{a})$$

This time we have E_m coefficients that will depend of the boundary conditions. How to determine the latter?

From the previous deflections we get the derivatives: $(\frac{\partial w_1}{\partial y})_{y=\pm a/2}$,$(\frac{\partial w_1}{\partial x})_{x=\pm a/2}$, $(\frac{\partial w_2}{\partial y})_{y=\pm a/2}$ and $(\frac{\partial w_2}{\partial x})_{x=\pm a/2}$.

And we use the boundary conditions to end up with a system to solve for E_m presented in equation (17):

$$(\frac{\partial w}{\partial y})_{y=\pm a/2} = 0 \Rightarrow (\frac{\partial w_1}{\partial y})_{y=\pm a/2} + (\frac{\partial w_2}{\partial y})_{y=\pm a/2} = 0$$

$$\text{and } (\frac{\partial w}{\partial x})_{x=\pm a/2} = 0 \Rightarrow (\frac{\partial w_1}{\partial x})_{x=\pm a/2} + (\frac{\partial w_2}{\partial x})_{x=\pm a/2} = 0$$

$$\Rightarrow \frac{E_i}{i}(tanh\alpha_i + \frac{\alpha_i}{cosh^2\alpha_i}) + \frac{8i}{\pi} \sum_{m=1,3,5...}^{\infty} \frac{E_m}{m^3} \frac{1}{(1 + \frac{i^2}{m^2})^2} = \frac{4qa^2}{\pi^3}\frac{1}{i^4}(-tanh\alpha_i + \frac{\alpha_i}{cosh^2\alpha_i}) \quad (17)$$

We can then solve for n number of coefficient the values for E_m by taking i from 1 to $2n+1$ in the equation above (i being odd as m). Indeed, by using numerical values for the various parameters we can end up with a system presented below (here we took the example where we consider only the first four term coefficients and the smallest coefficients have been neglected see [9]):

$$1.8033E_1 = 0.6677K$$
$$0.0764E_1 + 0.4045E_3 = 0.01232K$$
$$0.0188E_1 + 0.0330E_3 + 0.2255E_5 = 0.00160K$$
$$0.0071E_1 + 0.0159E_3 + 0.0163E_5 + 0.1558E_7 = 0.00042K$$

Where: $K = -4qa^2/\pi^3$. We finally compute $w = w_1 + w_2$ by incorporating the E_m coefficients in w_2.

We can see here that to go to n terms we will have to solve a $n \times n$ system for each material properties or mechanical boundaries considered. We will therefore present in the next section a simpler and more precise approach which is the Galerkin variational solution.

2.2.2 Variational methods

We will present here the method that will be implemented in the project to solve the problem. To do so, we chose to use the Galerkin method. By looking at the mathematical literature [7] we can see that our PDE (5) fulfills all the conditions to allow us to apply this method. Indeed, the Galerkin method can be used to approximate the solution to ordinary differential equations and partial differential equations making it is useful in solving almost all engineering problems with prescribed boundary conditions. The Galerkin method uses trial functions with a number of unknown parameters fitting the boundary conditions. Then the unknown parameters are determined by minimizing the error.

The Galerkin method is therefore a variational method of weighted residuals. Suppose we have a linear differential operator D acting on a function w to produce a function q then:
$D(w(x,y)) = q(x,y)$

The function w is in this method approximated by considering it as a linear combination of trial functions such that:

$w \simeq \tilde{w} = \sum_{i=1}^{n} a_i \phi_i(x,y)$

When used into the differential operator, D, the result of the operations is not in general $q(x,y)$ because an error residual will appear:

$R(x,y) = D(\tilde{w}(x,y)) - q(x,y) \neq 0 \Leftrightarrow R(x,y) = \sum_{i=1}^{n} a_i D(\phi_i(x,y)) - q(x,y)$

A Method of Weighted Residuals is where the residual over the domain is forced to be zero. In the case of our Galerkin method we therefore look at a_i coefficients such that:

$$\int_{Area} R(x,y)\phi_i dA = 0 \tag{18}$$

The ϕ_i trial functions can take various form (trigonometric [8], polynomial [5]...) as long as it fits the boundary conditions. The increase in the number of term of $\tilde{w}$ will increase precision but will however increase computational time to find the a_i coefficient forcing the residual to zero over the domain.

We chose to solve the problem using polynomial trial functions. Therefore, by applying this method to the PDE (5) and by using the boundary conditions:

$$\begin{cases} w = 0 & , x = \pm a/2 \\ w = 0 & , y = \pm a/2 \\ \frac{\partial w}{\partial x} = 0 & , x = \pm a/2 \\ \frac{\partial w}{\partial y} = 0 & , y = \pm a/2 \end{cases} \tag{19}$$

We can define trial polynomials (at least of degree 8, degree 4 in x and 4 in y due to the 8 symmetrical boundary conditions). We will therefore propose three orders of trial functions going increasingly in precision and in computational time.

First as presented above, we define a typical deflection satisfying the boundary conditions such that:

$$w \simeq \tilde{w_{kl}} = \sum_{k=0}^{\infty}\sum_{l=0}^{\infty} a_{kl}\phi_{kl} = (x^2 - \frac{a^2}{4})^2(y^2 - \frac{a^2}{4})^2 \sum_{k=0}^{\infty}\sum_{l=0}^{\infty} a_{kl}x^k y^l \tag{20}$$

For the first order method we define the following trial function:

$$\tilde{w_1} = a_{00}\phi_{00} \tag{21}$$

We then have to solve a_{00} for the residuals:

$$\int_{Area} (\frac{\partial^4 \tilde{w_1}}{\partial x^4} + \frac{\partial^4 \tilde{w_1}}{\partial y^4} + 2\frac{\partial^4 \tilde{w_1}}{\partial x^2 \partial y^2} - \frac{q}{D})\phi_{00} dA = 0 \tag{22}$$

For the second order we have:

$$\tilde{w_2} = a_{00}\phi_{00} + a_{20}\phi_{20} + a_{02}\phi_{02} \tag{23}$$

We then have to solve a_{00},a_{20} and a_{02} for the residuals:

$$\begin{cases} \int_{Area}(\frac{\partial^4\tilde{w_2}}{\partial x^4}+\frac{\partial^4\tilde{w_2}}{\partial y^4}+2\frac{\partial^4\tilde{w_2}}{\partial x^2\partial y^2}-\frac{q}{D})\phi_{00}dA=0 \\ \int_{Area}(\frac{\partial^4\tilde{w_2}}{\partial x^4}+\frac{\partial^4\tilde{w_2}}{\partial y^4}+2\frac{\partial^4\tilde{w_2}}{\partial x^2\partial y^2}-\frac{q}{D})\phi_{20}dA=0 \\ \int_{Area}(\frac{\partial^4\tilde{w_2}}{\partial x^4}+\frac{\partial^4\tilde{w_2}}{\partial y^4}+2\frac{\partial^4\tilde{w_2}}{\partial x^2\partial y^2}-\frac{q}{D})\phi_{02}dA=0 \end{cases} \tag{24}$$

Finally, the third order deflection can be written as:

$$\tilde{w_3}=a_{00}\phi_{00}+a_{20}\phi_{20}+a_{02}\phi_{02}+a_{40}\phi_{40}+a_{04}\phi_{04}+a_{22}\phi_{22} \tag{25}$$

We then have to solve a_{00},a_{20}, a_{02}, a_{40}, a_{04} and a_{22} for the residuals:

$$\begin{cases} \int_{Area}(\frac{\partial^4\tilde{w_3}}{\partial x^4}+\frac{\partial^4\tilde{w_3}}{\partial y^4}+2\frac{\partial^4\tilde{w_3}}{\partial x^2\partial y^2}-\frac{q}{D})\phi_{00}dA=0 \\ \int_{Area}(\frac{\partial^4\tilde{w_3}}{\partial x^4}+\frac{\partial^4\tilde{w_3}}{\partial y^4}+2\frac{\partial^4\tilde{w_3}}{\partial x^2\partial y^2}-\frac{q}{D})\phi_{20}dA=0 \\ \int_{Area}(\frac{\partial^4\tilde{w_3}}{\partial x^4}+\frac{\partial^4\tilde{w_3}}{\partial y^4}+2\frac{\partial^4\tilde{w_3}}{\partial x^2\partial y^2}-\frac{q}{D})\phi_{02}dA=0 \\ \int_{Area}(\frac{\partial^4\tilde{w_3}}{\partial x^4}+\frac{\partial^4\tilde{w_3}}{\partial y^4}+2\frac{\partial^4\tilde{w_3}}{\partial x^2\partial y^2}-\frac{q}{D})\phi_{04}dA=0 \\ \int_{Area}(\frac{\partial^4\tilde{w_3}}{\partial x^4}+\frac{\partial^4\tilde{w_3}}{\partial y^4}+2\frac{\partial^4\tilde{w_3}}{\partial x^2\partial y^2}-\frac{q}{D})\phi_{40}dA=0 \\ \int_{Area}(\frac{\partial^4\tilde{w_3}}{\partial x^4}+\frac{\partial^4\tilde{w_3}}{\partial y^4}+2\frac{\partial^4\tilde{w_3}}{\partial x^2\partial y^2}-\frac{q}{D})\phi_{22}dA=0 \end{cases} \tag{26}$$

NB: ϕ_{kl} are defined as in equation (20) and we therefore have:

$\phi_{00}=(x^2-\frac{a^2}{4})^2(y^2-\frac{a^2}{4})^2$,$\phi_{20}=(x^2-\frac{a^2}{4})^2(y^2-\frac{a^2}{4})^2x^2$,$\phi_{02}=(x^2-\frac{a^2}{4})^2(y^2-\frac{a^2}{4})^2y^2$,$\phi_{40}=(x^2-\frac{a^2}{4})^2(y^2-\frac{a^2}{4})^2x^4$,$\phi_{04}=(x^2-\frac{a^2}{4})^2(y^2-\frac{a^2}{4})^2y^4$ and $\phi_{22}=(x^2-\frac{a^2}{4})^2(y^2-\frac{a^2}{4})^2y^2x^2$

Now, that we have chosen our trial function for deflection we have to find the a_{kl} coefficients forcing the residuals to zero over the area. To do so, we will use the symbolic algebraic software Mathematica. The implementation allowing the resolution of the problem through Mathematica will be presented in the next section.

3 Implementation and results

3.1 Circular plate

For the circular plate we can directly use the result from the equation (15) to try to find the sign of the electric displacement D_z over the area. By looking at the equation (10) we can see that the function's sign to be studied is: $T_{rr}+T_{\theta\theta}$. Besides, by using the result of (15) we can see that:

$$T_{rr}+T_{\theta\theta}>0 \Leftrightarrow a^2-2r^2>0 \Leftrightarrow 1-2R^2>0 \text{ where } R=r/a$$

We use the latter adimensional variable to compute the deflection and electrical displacement adimentionalized functions. Those functions are illustrated in figure 5.

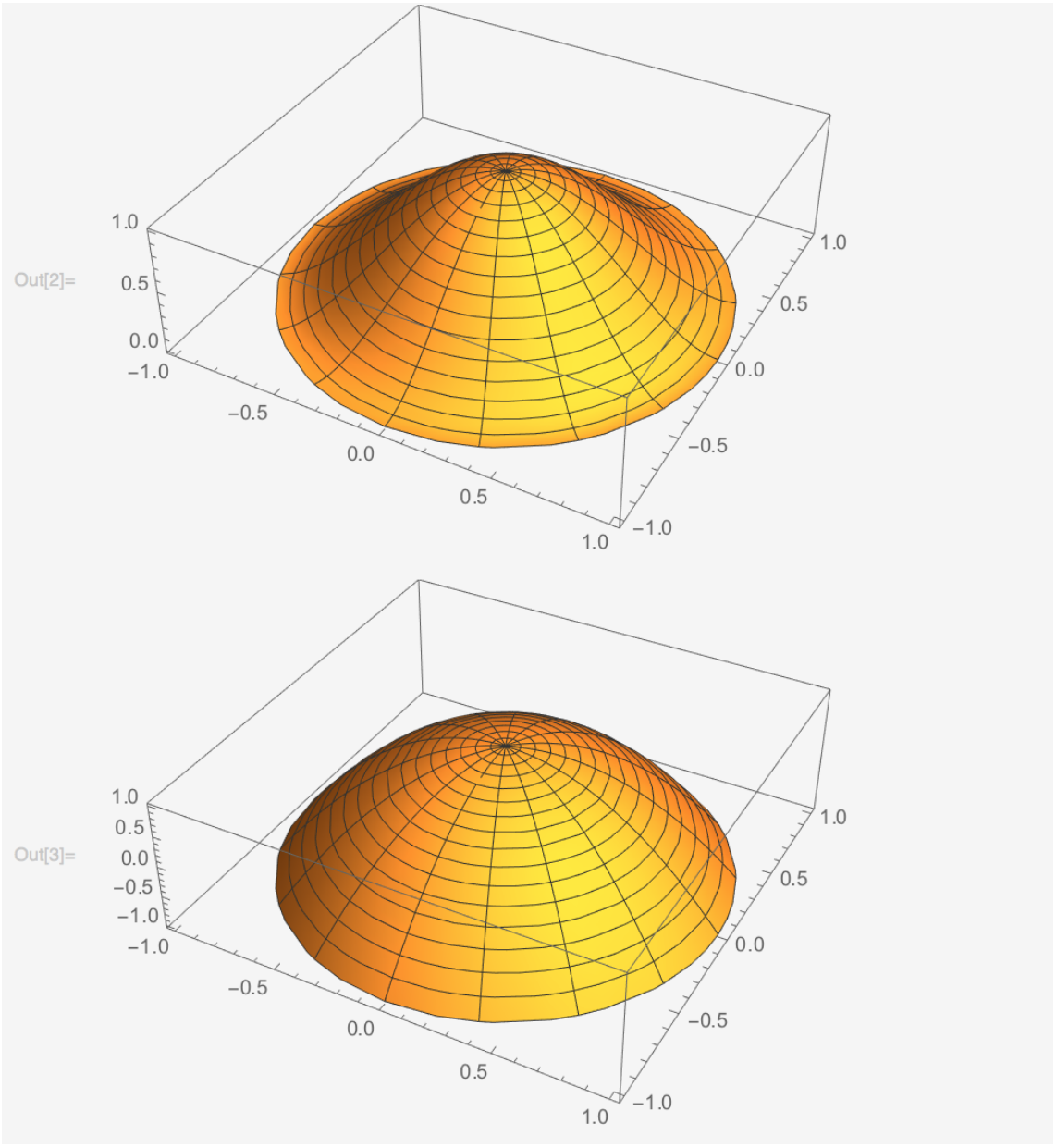

Figure 5: Top to bottom are computed the deflection and total stress functions obtained for a circular plate

Finally, the identified areas of opposite signs for D_z are illustrated in figure 6:

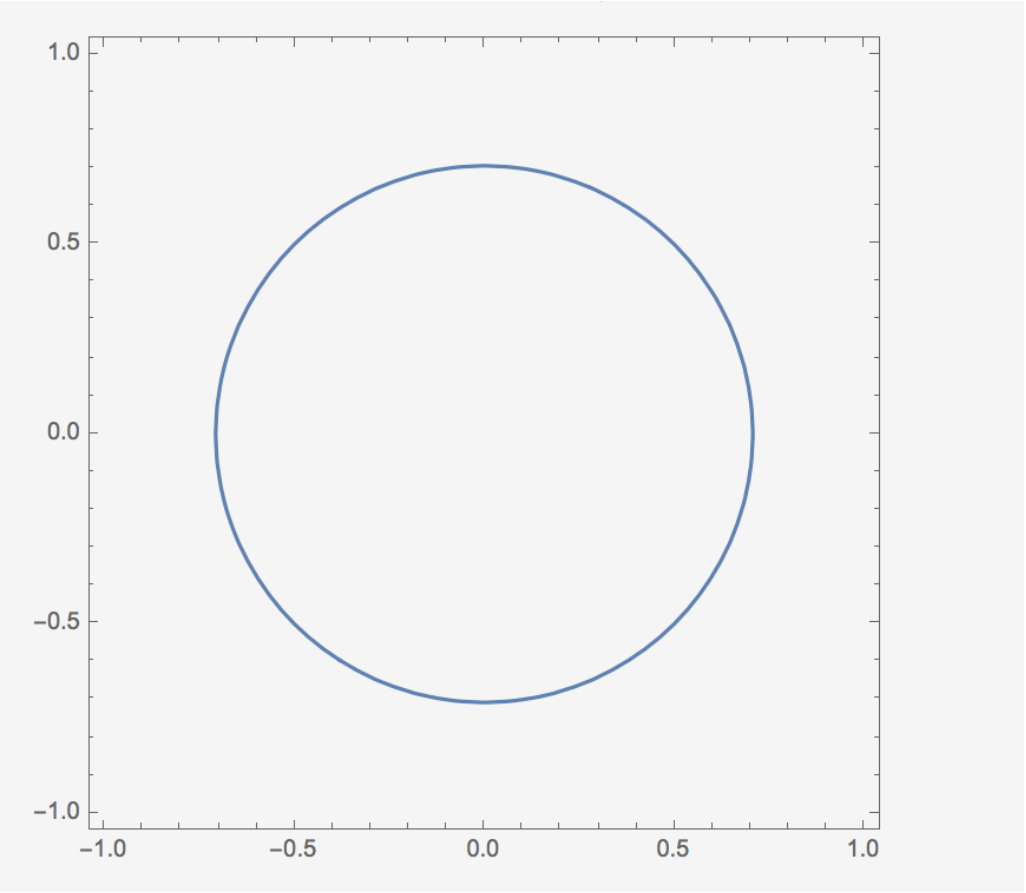

Figure 6: Areas delimitation

NB: The figure presented above has been obtained by using cartesian coordinate using the following code:

```
%We define the poisson ratio that however does not enter into account in St sign

nu=0.3;


%The normalized deflection is rewritten with cartesian coordinates

w=(1-x^2-y^2)^2;


%The derivatives required to find stresses are computed

d2x = D[w, {x, 2}]; d2y=D[w, {y, 2}]; dxy= D[w, x, y];


%Here we only compute the part of the stress that influences it sign

Txx = Simplify [(d2x+nu*d2y)];
Tyy = Simplify [(nu*d2x+d2y)];

%St determines the sign of Dz the electrical displacement
Tt=Txx+Tyy;
ContourPlot[{St==0},{y, -1,1}, {x, -1,1}]
```

Indeed, to verify the equation considered for D_z (10) with the same d_{31} due to isotropy we

rewrote the deflection from equation (13) in cartesian coordinates (with $r = \sqrt{x^2 + y^2}$) and we computed new stresses T_1 and T_2 using equation 8). The new D_3/d_{31} has then be compared to D_z/d_{31} and the functions where found to be exactly identical.

We therefore have the the circle of radius $\frac{\sqrt{2}}{2}a$ with the same center of our plate that delimits the two areas we wanted to distinguish.

3.2 Square plate

3.2.1 Implementation [1]

Here we will try to determine the a_{kl} coefficients presented in section 2.2.2. However, by looking at the different residuals eq.(24),(25) and (26) we can see that many symbolic parameters are involved such as a length of the square for the integral boundaries and q/D making the computation of the a_{kl} coefficients almost impossible. We therefore decided to simplify the equation to be solved by adimentionalizing the governing equation for the deflection as follow.

First we define two new variables ξ and η such that:

$$\xi = \frac{x}{a} \text{ and } \eta = \frac{y}{a}$$

Therefore:

$$(16) \Leftrightarrow \frac{\partial^4 w}{\partial \xi^4} + \frac{\partial^4 w}{\partial \eta^4} + 2\frac{\partial^4 w}{\partial \xi^2 \partial \eta^2} = \frac{qa^4}{D}$$

And:

$$(19) \Leftrightarrow \begin{cases} w = 0 & ,\xi = \pm 1/2 \\ w = 0 & ,\eta = \pm 1/2 \\ \frac{\partial w}{\partial \xi} = 0 & ,\xi = \pm 1/2 \\ \frac{\partial w}{\partial \eta} = 0 & ,\eta = \pm 1/2 \end{cases}$$

Therefore, the boundaries of the integral are no longer symbolic.

Besides, by choosing to solve the residuals equation for a certain ratio $\frac{qa^4}{D}$ the computational time becomes much faster. We choose here arbitrarily to continue with $\frac{qa^4}{D} = 1$. This means for example that the problem for the first order becomes finding a_{00} such that:

$$\tilde{w_1} = a_{00}\phi_{00} \tag{27}$$

With:

$$\phi_{00} = (x^2 - \tfrac{1}{4})^2(y^2 - \tfrac{1}{4})^2$$

And:

$$\int_{-1/2}^{1/2}\int_{-1/2}^{1/2}(\frac{\partial^4 \tilde{w_1}}{\partial \xi^4} + \frac{\partial^4 \tilde{w_1}}{\partial \eta^4} + 2\frac{\partial^4 \tilde{w_1}}{\partial \xi^2 \partial \eta^2} - 1)\phi_{00} d\xi d\eta = 0 \tag{28}$$

We will therefore present the three codes for the three orders presented in section 2.2.2 followed by the found deflections $\tilde{w_{1,2,3}}$.

To solve for the first order we use the following code:

```
1
%We first specify the trial function
3
phi = Expand [ (x^2 - 1/4) ^2 * (y^2 - 1/4)
5 ^2];
w=a00 * phi;
7
%We evaluate the Galerkin integral
9
GalInt=Simplify [Integrate  [(D [w, {x, 4}]+
11 2* D [w, {x, 2}, {y, 2}] +
D [w, {y, 4} ] - 1 )*phi,
```

```
{x, -1/2, 1/2},{y, -1/2, 1/2}]] ;

%We solve the Galerkin equation for a00

Galsol = Simplify [Solve [GalInt == 0, a00 ] ];

%We evaluate the deflection

w = Simplify [w /. Galsol]
```

We get for the deflection:

$$\tilde{w_1} = (5(1-4\xi^2)^2(1-4\eta^2)^2)/2048 \tag{29}$$

To solve for the second order we use the following code:

```
%We first specify the trial functions

phif = Expand [ (x^2 - 1/4) ^2 * (y^2 - 1/4)
^2];

w = a00*phif+a20*phif*x^2+a02*phif*y^2 ;

%We evaluate the Galerkin integrals

GalInt1=Simplify [Integrate  [(D [w, {x, 4}]+
2* D [w, {x, 2}, {y, 2}] +
D [w, {y, 4} ] - 1 )* phif,
{x, -1/2, 1/2},{y, -1/2, 1/2}]] ;

GalInt2=Simplify [Integrate  [(D [w, {x, 4}]+
2* D [w, {x, 2}, {y, 2}] +
D [w, {y, 4} ] - 1 )* phif*x^2,
{x, -1/2, 1/2},{y, -1/2, 1/2}]] ;

GalInt3=Simplify [Integrate  [(D [w, {x, 4}]+
2* D [w, {x, 2}, {y, 2}] +
D [w, {y, 4} ] - 1 )* phif*y^2,
{x, -1/2, 1/2},{y, -1/2, 1/2}]] ;

%We solve the Galerkin system for a00,a20,a02

Galsol =Simplify [Solve [{GalInt1==0, GalInt2==0,GalInt3==0},{a00,a02,a20}]];

%We evaluate the deflection

w = Simplify [w /. Galsol]
```

We get for the deflection:

$$\tilde{w_2} = (77(1-4\xi^2)^2(1-4\eta^2)^2(269+312\xi^2+312\eta^2))/16404480 \tag{30}$$

To solve for the third order we use the following code:

```


%We first specify the trial function

phif = Expand [ (x^2 - 1/4) ^2 * (y^2 - 1/4)
^2];

w = a00*phif+a20*phif*x^2+a02*phif*y^2+a40*phif*x^4+a04*phif*y^4+a22*phif*x^2*y^2 ;

%We evaluate the Galerkin integrals

GalInt1=Simplify [Integrate  [(D [w, {x, 4}]+
```

```
2* D [w, {x, 2}, {y, 2}] +
D [w, {y, 4} ] - 1 )* phif,
{x, -1/2, 1/2},{y, -1/2, 1/2}]] ;

GalInt2=Simplify [Integrate  [(D [w, {x, 4}]+
2* D [w, {x, 2}, {y, 2}] +
D [w, {y, 4} ] - 1 )* phif*x^2,
{x, -1/2, 1/2},{y, -1/2, 1/2}]] ;

GalInt3=Simplify [Integrate  [(D [w, {x, 4}]+
2* D [w, {x, 2}, {y, 2}] +
D [w, {y, 4} ] - 1 )*phif*y^2,
{x, -1/2, 1/2},{y, -1/2, 1/2}]] ;

GalInt4=Simplify [Integrate  [(D [w, {x, 4}]+
2* D [w, {x, 2}, {y, 2}] +
D [w, {y, 4} ] - 1 )* phif*x^4,
{x, -1/2, 1/2},{y, -1/2, 1/2}]] ;

GalInt5=Simplify [Integrate  [(D [w, {x, 4}]+
2* D [w, {x, 2}, {y, 2}] +
D [w, {y, 4} ] - 1 )* phif*y^4,
{x, -1/2, 1/2},{y, -1/2, 1/2}]] ;

GalInt6=Simplify [Integrate  [(D [w, {x, 4}]+
2* D [w, {x, 2}, {y, 2}] +
D [w, {y, 4} ] - 1 )* phif*y^2*x^2,
{x, -1/2, 1/2},{y, -1/2, 1/2}]] ;

%We solve the Galerkin system for a00,a20,a02,a40,a04 and a22

Galsol =Simplify [Solve [{GalInt1==0, GalInt2==0,GalInt3==0, GalInt4==0, GalInt5
    ==0, GalInt6==0},{a00,a20,a02,a40,a04,a22}]];

%We evaluate the deflection


w = Simplify [w /. Galsol]
```

We get for the deflection:

$$\tilde{w_3} = 1/18022968008704429(1-4\xi^2)^2(1-4\eta^2)^2 \\ (53162867 + 11564080\xi^4 + 54681404\eta^2 + 11564080\eta^4 + \\ 4\xi^2(13670351 + 65341012\eta^2)) \tag{31}$$

We then compute the plate response as follow:

```
%We compute the required derivatives of th deflection

d2x = D[w, {x, 2}]; d2y=D[w, {y, 2}]; dxy= D[w, x, y];
nu=0.3;

%The momentums, forces and stresses are defined

Mx = Simplify [ - (flex*\.03d2x + flex* nu*d2y) ];
My = Simplify [ - (flex*nu*\.03d2x + flex \.03*d2y) ];
Mxy = Simplify [ - 2*\.03flex*(1-nu) *dxy/2]
Qx = Simplify [ - (flex \.03*D [d2x, x] + flex*\.03D [d2y,
x]) ];
Qy = Simplify [ - (flex \.03*D [d2x, y] + flex \.03*D [d2y,
y]) ];

%NB: We only use here the components of the stress that affect its sign

Txx = Simplify [(d2x+nu*d2y)]
Tyy = Simplify [(nu*d2x+d2y)]
Txy = Simplify [(1-nu) *dxy];

```

```
%Electric field displacement

D3=d31*(Txx+Tyy);
```

By integrating this D_3 function over the whole area we get zero meaning that the positive and negative stresses over the plate are equally important emphasizing the importance of being able to distinguish their respective domains.

3.2.2 Results

We first compared the deflections found for each order in order to quantify the improvement. To do so, we define a relative error function e_1 such that:

$$e_{1ij} = \frac{\left|w_i - w_j\right|}{\left|w_i\right|}$$

And another relative error e_2 function such that:

$$e_{2ij} = \frac{\left|\frac{\partial^2 \tilde{w_i}}{\partial \eta^2} - \frac{\partial^2 \tilde{w_j}}{\partial \eta^2}\right|}{\left|\frac{\partial^2 \tilde{w_i}}{\partial \eta^2}\right|}$$

We then find the maximum value of e_1 and e_2 over the area with the Mathematica tool :"FindMaxValue". We can present the matrices e_1 and e_2 obtained:

$$e_1 = \begin{pmatrix} 0 & & \\ 0.15 & 0 & \\ 0.15 & 0.02 & 0 \end{pmatrix} \tag{32}$$

And:

$$e_2 = \begin{pmatrix} 0 & & \\ 0.23 & 0 & \\ 0.21 & 0.06 & 0 \end{pmatrix} \tag{33}$$

We can see that the difference for the deflection between the first order and the two others is drastic. Besides, although the maximal difference between the second and the third order deflections is under 2%, we can see that it becomes high (6%) for the difference between their second derivatives and since the stress involves the second derivative, we decided to choose the third order for the rest of the study.

We can now present the deflection and stresses obtained for this third order (see figure 7):

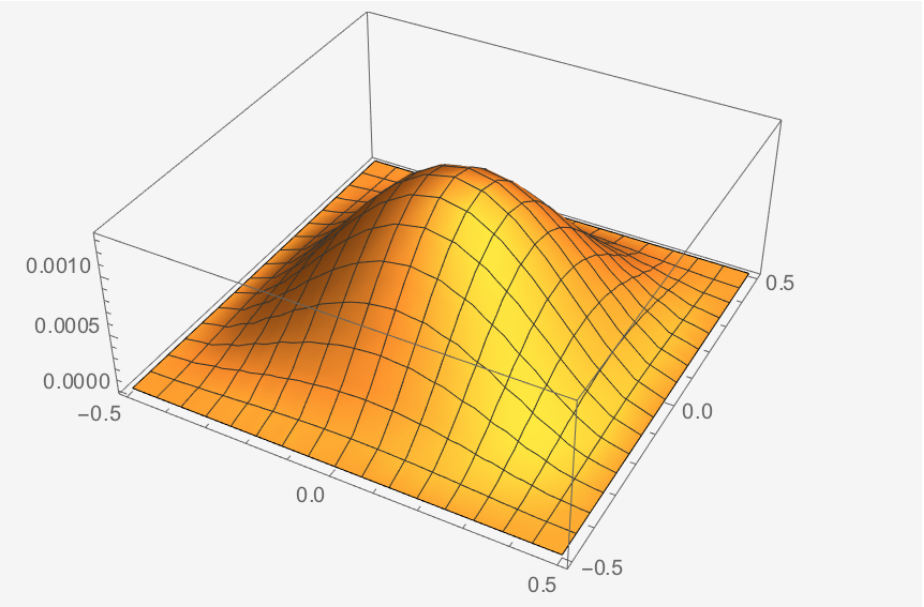

(a) Deflection for a square plate

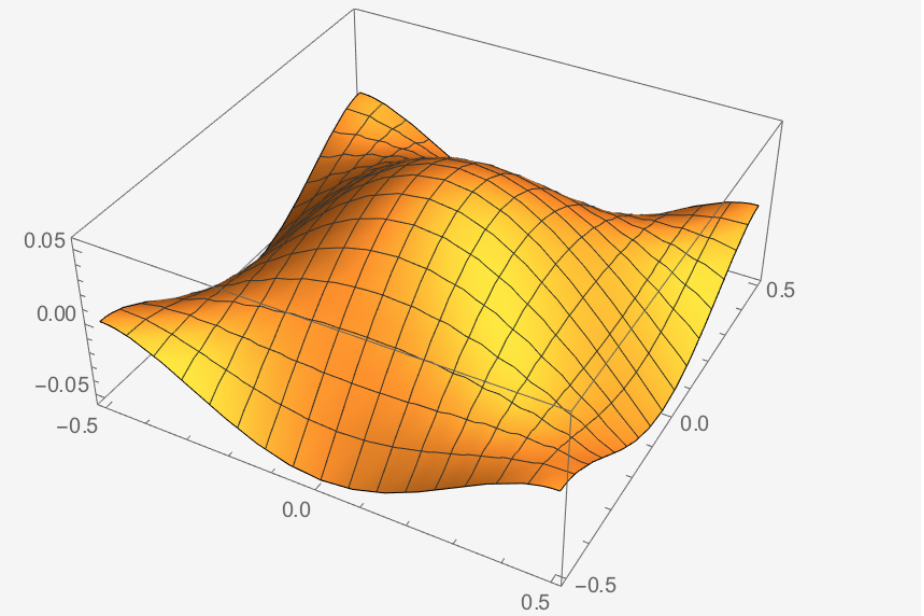

(b) Total stress $T_1 + T_2$ for a square plate

Figure 7: Results for the third order polynomial trial functions

We also decided to solve the problem using a finite element software (Ansys) to verify the validity of our results. A structural Ansys analysis is done by the following procedure. The Ansys system has six different states:

1. Engineering Data
2. Geometry
3. Model
4. Setup
5. Solution
6. Results

The Engineering Data cell gives access to the material models for the use in the analysis. We note here the value of the flexural rigidity D for the used material and we make sure that the used

material is isotropic.

For the geometry we define a square of 1m side and 0.1m width. Indeed, the objective here is to be able to compare the result in Ansys with the variational method solution obtained above. Therefore, we will chose the a length here and the load q latter on such that the coefficient: $\frac{qa^4}{D} = 1$.

The mesh is then defined applying the proximity and curvature refinement.

The setup option is used to launch the appropriate application for the system. Here we define the boundary conditions and configure the analysis in the system. We put the fully clamped constraints along the lateral surface of our plate and we apply an uniformly distributed pressure normal to the surface on the top surface such that $\frac{qa^4}{D} = 1$.

For the solution and result we chose to present the normal deformation on the top surface and one of the in-plane internal stresses. Indeed, by computing T_{12} we observed that the latter was negligible compared to T_{11} and T_{22}. Therefore, the T matrix is almost diagonal and thus it makes sens to compare the principal stresses from Ansys from the T_{11} and T_{22} stresses we have computed. Besides, due to the symmetry of the problem, we only have to compare for one of the two stresses. We therefore present the T_1 stress obtained from the third order approximation in the figure 8 below:

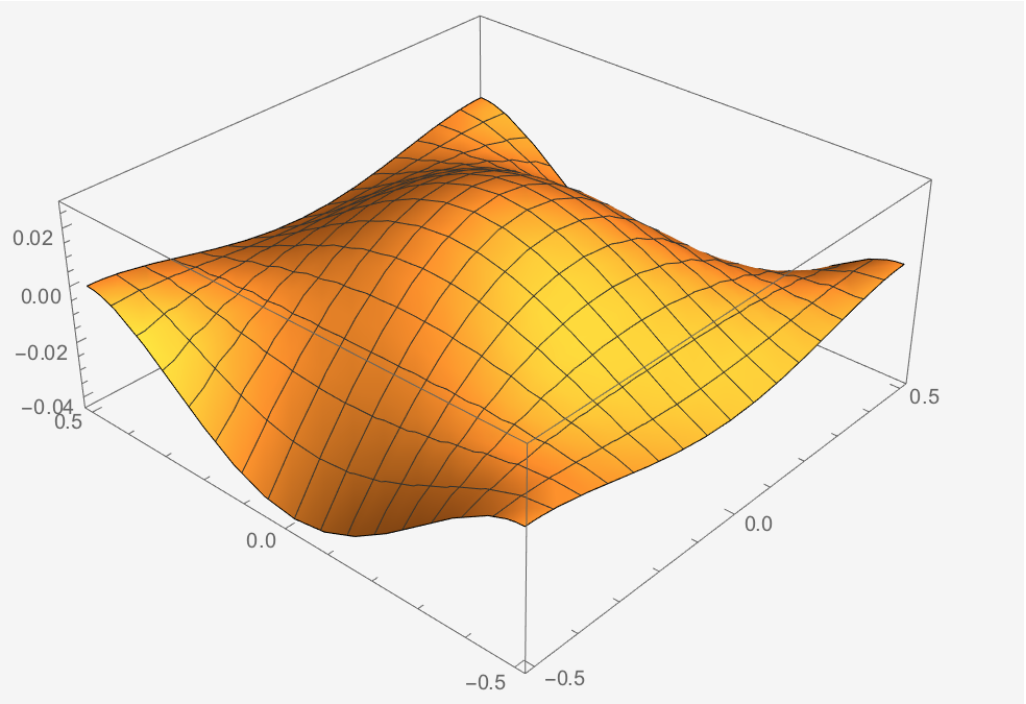

Figure 8: T_1 stress for a square plate (third order solution)

Finally, we present on figure 9 the finite element solution.

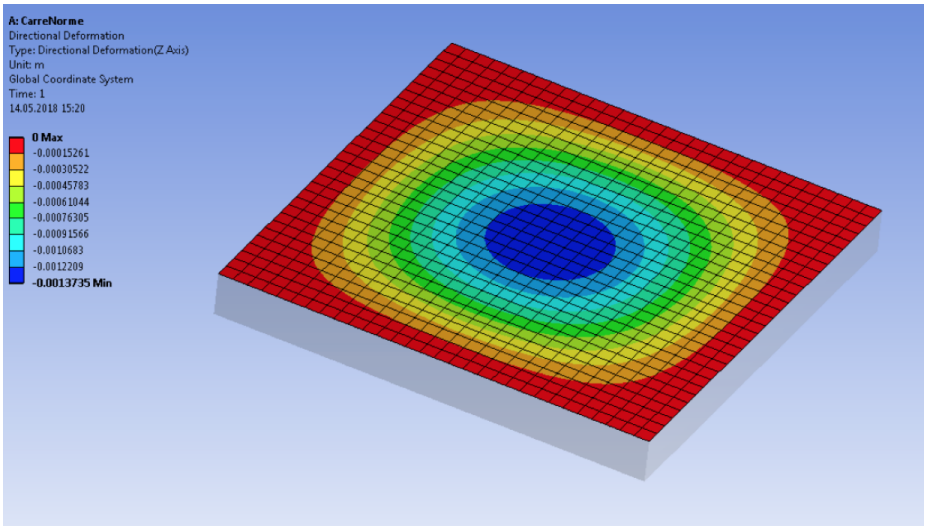

(a) Deflection normal to the plate

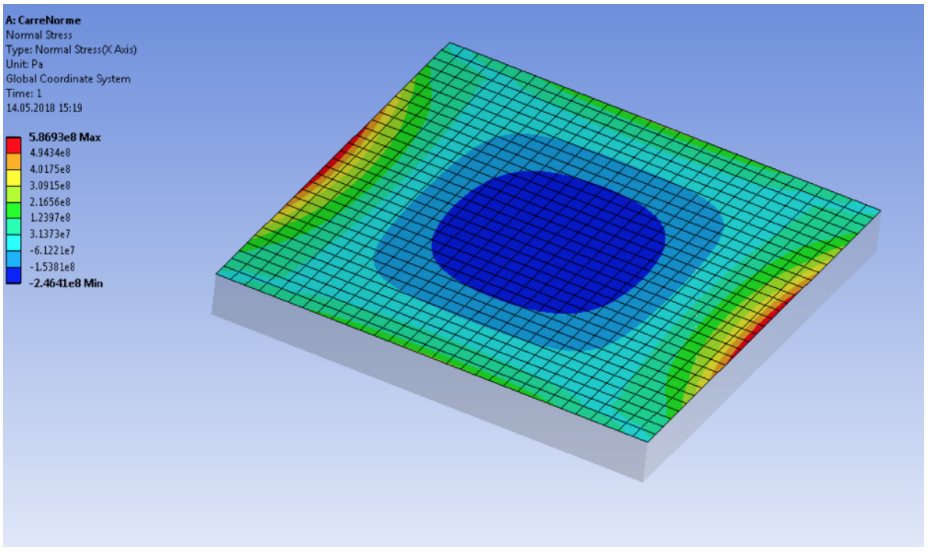

(b) Principal stress along x-axis

Figure 9: Square plate finite elements solution

NB: We cannot directly compare the numerical values for the stresses from figure 9 and 8 since the T_1 from figure 8 has been obtained with:

```
Txy = Simplify [(1-nu) *dxy];
```

Where the coefficient $\frac{-12Dz}{h^3}$ from equation (8) does not appear.

By comparing the finite element solution with our polynomial solution we found that the value of the maximum deflection of the flat square plate is 0.0013735, which shows good agreement with the value determined by the analytical method (2% difference). Besides, we can see that the two functions for the stresses observe the same variations which is crucial to determine the sign of the total stress $T_1 + T_2$.

Finally, we use the following code to distinguish the positive/negative domains of the electrical displacement:

```
d2x = D[w, {x, 2}]; d2y=D[w, {y, 2}]; dxy= D[w, x, y];
```

```
Txx = Simplify [(d2x+nu*d2yr)];
Tyy = Simplify [(nu*d2x+d2yr)];
Txy = Simplify [-(12*flex*z/H^3)*(1-nu) *dxy];

%Total stress that determines D3 sign

Tt=Txx+Tyy;

%Contour plot to delimit positive/negative domains

ContourPlot[{Tt==0},{x,-1/2, 1/2}, {y, -1/2,1/2}]

%Exact analytical solution to define the delimitation

Reduce[Tt>0 && 0< y< 0.5 && 0<x<0.5 ,y]
Reduce[Tt<0 && 0< y< 0.5 && 0<x<0.5 ,y]
```

The result we get is presented in the figure 10 below:

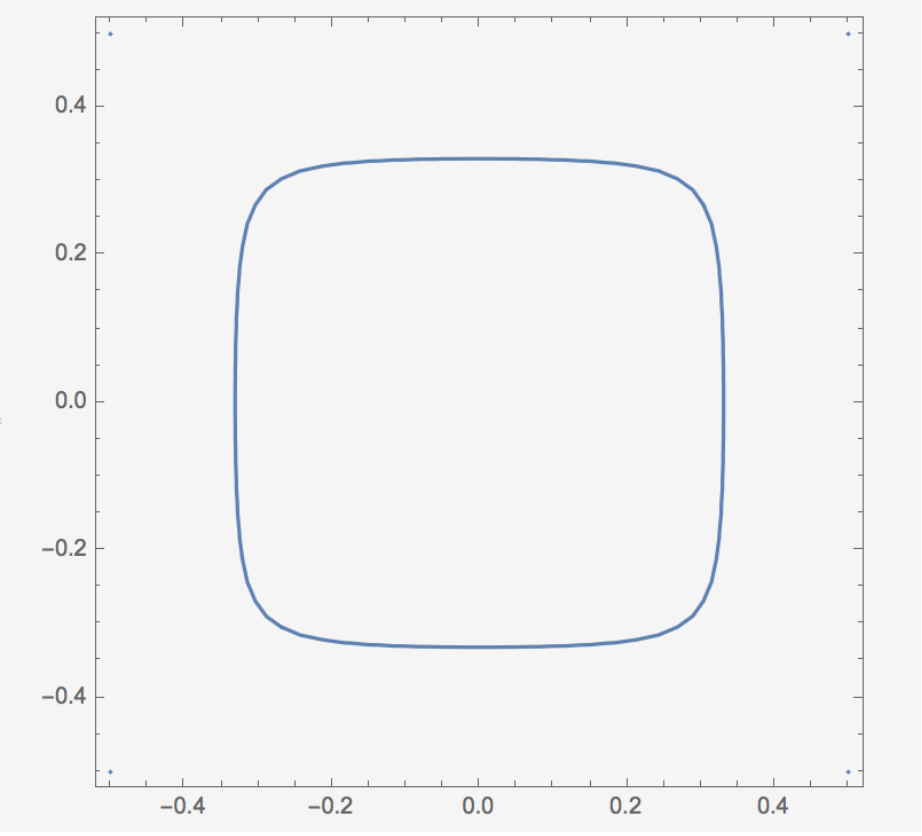

(a) Positive/negative electrical displacement areas delimitation

$$(0 < x < 0.288675 \&\& \text{Root}[-1. + 10.\,x^2 - 8.\,x^4 + (10. - 96.\,x^2 + 96.\,x^4)\,\#1^2 + (-8. + 96.\,x^2)\,\#1^4 \&,\, 3] < y < 0.5) \;||\; (0.288675 \le x < 0.331077 \&\& \text{Root}[-1. + 10.\,x^2 - 8.\,x^4 + (10. - 96.\,x^2 + 96.\,x^4)\,\#1^2 + (-8. + 96.\,x^2)\,\#1^4 \&,\, 2] < y < 0.5) \;||\; (0.331077 \le x < 0.5 \&\& 0 < y < 0.5)$$

(b) Exact analytical delimitation of the positive domain

Figure 10: Square Positive/negative electrical displacement areas delimitations

4 Conclusion

We solved the sign study of the electrical displacement over the plate area. On the one hand, an analytical solution was derived for the circular plate and the exact positive/negative domains of the plate were identified. On the other hand, for the square plate, a variational approach using Galerkin method was introduced. The involved algebra was managed using the symbolic software, Mathematica. The method has been led by selecting polynomials satisfying all the boundary conditions and provides better accuracy and faster convergence than direct method involving infinite series. The use of the symbolic software provided therefore a much faster and accurate way of analyzing the engineering problem. Besides, we have shown throughout this project that the results generated by the symbolic software shows good agreement with those of the finite element software, Ansys. However, the limitation of this approach is that the coefficients forcing the residual to zero over the plate area have to be recalculated each time we consider a new $\frac{qa^4}{D}$ ratio. Finally, it could have been interesting to see the limitations of our numerous assumptions (isotropy, flat plate, small deformation, in-plane stresses...) by experimental testing. However, the area that have been determined are very easy to identify and the delimitation should not be hard to define in order to optimize the electrical response detection.

References

[1] Abraham I Beltzer. *Variational and finite element methods: A symbolic computation approach.* Springer Science & Business Media, 2012.

[2] Gary K Fedder, Christofer Hierold, Jan G Korvink, and Osamu Tabata. *Resonant mems: Fundamentals, implementation, and application.* John Wiley & Sons, 2015.

[3] AL Kholkin, NA Pertsev, and AV Goltsev. Piezoelectricity and crystal symmetry. In *Piezoelectric and Acoustic Materials for Transducer Applications*, pages 17–38. Springer, 2008.

[4] Robert John Littrell. *High performance piezoelectric MEMS microphones.* PhD thesis, University of Michigan, 2010.

[5] Osadebe N. N and Aginam C. H. Bending analysis of isotropic rectangular plate with all edges clamped: Variational symbolic solution. *Journal of Emerging Trends in Engineering and Applied Sciences (JETEAS) 2 (5): 846-852(ISSN: 2141-7016) 846*, 2011.

[6] R Selvamani and P Ponnusamy. Elasto dynamic wave propagation in a transversely isotropic piezoelectric circular plate immersed in fluid. *Materials Physics and Mechanics*, 17(2):164–177, 2013.

[7] K Stewartson. Variational methods in mathematical physics, 1966.

[8] Robert L Taylor and Sanjay Govindjee. Solution of clamped rectangular plate problems. *International Journal for Numerical Methods in Biomedical Engineering*, 20(10):757–765, 2004.

[9] Stephen P Timoshenko and Sergius Woinowsky-Krieger. *Theory of plates and shells.* McGraw-hill, 1959.

[10] Matthew D Williams. *Development of a MEMS piezoelectric microphone for aeroacoustic applications.* PhD thesis, University of Florida, 2011.

[11] Warren C Young and Richard G Budnyas. *Roark's formulas for stress and strain.* McGraw-Hill, 2017.